Geol. Mag. **144** (*4*), *2007, pp. 643–659.* © *2007 Cambridge University Press*
doi:10.1017/S0016756807003470 First published online 29 May 2007 *Printed in the United Kingdom*

Hybrid magma generation preceding Plinian silicic eruptions at Hekla, Iceland: evidence from mineralogy and chemistry of two zoned deposits

GUDRUN SVERRISDOTTIR*

Nordic Volcanological Center, Institute of Earth Sciences, University of Iceland, Sturlugata 7, 101 Reykjavik, Iceland

(*Received* 21 November 2005; *accepted* 9 November 2006)

Abstract – Hekla is a Holocene volcanic ridge in southern Iceland, which is notable for the link between repose periods and the composition of the first-erupted magma. The two largest explosive silicic eruptions, H4 and H3, erupted about 4200 and 3000 years ago. Airfall deposits from these eruptions were sampled in detail and analysed for major and trace elements, along with microprobe analyses of minerals and glasses. Both deposits show compositional variation ranging from 72 % to 56 % SiO_2, with mineralogical evidence of equilibrium crystallization in the early erupted rhyolitic component but disequilibrium in the later erupted basaltic andesite component. The eruptions started with production of rhyolitic magma followed by dacitic to basaltic andesite magma. Sparse crystallization of the intermediate magma and predominant reverse zoning of minerals, trending towards a common surface composition, indicate magma mixing between rhyolite and a basaltic andesite end-member. The suggested model involves partial melting of older tholeiitic crust to produce silicic magma, which segregated and accumulated in deep crustal reservoir. Silicic magma eruption is triggered by basaltic andesite dyke injection, with a proportion of the dyke magma contributing to the production and eruption of a mixed hybrid magma. Both the volume of the silicic partial melt, and the proportion of the hybrid magma depend on the pre-eruptive repose time.

Keywords: hybrid magma, magma mixing, magma chamber, zoned deposit.

1. Introduction

The large proportion of silicic magma produced by Icelandic central volcanoes is rare for oceanic ridge environments. Detailed studies of several volcanoes in Iceland (Kerlingarfjoll, Askja, Torfajökull, Krafla) have shed light on the processes producing the evolved magma, most of them involving some reworking of the crust (K. Gronvold, unpub. Ph.D. thesis, Univ. Oxford, 1972; Sigurdsson & Sparks, 1981; McGarvie *et al.* 1990; Gunnarsson, Marsh & Taylor, 1998; Jonasson, 1994). Rock suites of these volcanoes are predominantly bimodal, but Hekla produces a higher proportion of intermediate magma, from basaltic andesite to rhyolite, according to the terminology of Le Bas *et al.* (1986).

The volcanism of Hekla has been studied using tephrochronology and detailed historical records (Thorarinsson, 1967). The known dated eruptions are shown in Table 1, along with roughly estimated volumes. The SiO_2 content of the large eruptions generally exceeds 70 %, and only a minor proportion of erupted magma contains as little as 55 % SiO_2. The proportions are almost reverse for the smaller eruptions, where compositions are predominantly intermediate (ranging from 54 % to 63 % SiO_2). Compositional variation is seen in all erupted material except that from the last four eruptions since 1970. The most pronounced variation is found in the largest eruptions, with a range of 16 % SiO_2. Estimates based on calculations and approximations shown in Table 1 indicate that the basaltic andesite productivity of Hekla has increased in the past 1000 years.

Research on the chemistry and petrology of Hekla has been extensive, although key aspects remain poorly understood. Bunsen (1851) suggested that silicic and basaltic magmas were interacting beneath the volcano. Einarsson (1950) suggested differentiation of the Hekla magma by crystal fractionation. Tryggvason (1965) described the mineralogy and chemistry of the products, and Tomasson (1967) proposed two magma chambers beneath Hekla, and favoured mixing of silicic and basic magma to explain the chemical characteristics. Thorarinsson (1967) pointed out that the silica content of the initial phase of each eruption was proportional to the length of the repose period. Baldridge *et al.* (1973), in their study of the 1970 Hekla eruption, favoured fractional crystallization. Sigvaldason (1974) proposed mixing of two different magmas produced by crustal melting. Sigmarsson, Condomines & Fourcade (1992) made a detailed isotope study of Hekla products and showed that two unrelated magmas, assumed to have formed by partial melting of the deep crust, produced the rock suite by mixing and later modification by crystallization.

*Author for correspondence: gsv@hi.is

Table 1. Known Hekla eruptions

Eruption	Date	Dating method	km^3 DRE	References for volume estimate
H5	>7000 BP	Estimated	0.7	Larsen & Thorarinsson, 1977
H4	~4200 BP	Corr. ^{14}C	1.8	Larsen & Thorarinsson, 1977
H-Sv	~3900 BP	Corr. ^{14}C	0.4–0.5	Sverrisdottir (unpub. data)
H3	~3000 BP	Corr. ^{14}C	2.2	Larsen & Thorarinsson, 1977
HX ~15 eruptions	??		<0.5 × 15	B. Robertsdottir, pers. comm.
		Tephrochronology + historical records		
1104	AD	"	~0.5	Modified after Thorarinsson, 1967
1158	AD	"	~0.15	"
1206	AD	"	~0.15	"
1222	AD	"	~0.15	"
1300	AD	"	~0.57	"
1341	AD	"	~0.15	"
1389	AD	"	~0.25	"
1510	AD	"	~0.79	"
1597	AD	"	~0.56	"
1636	AD	"	~0.2	"
1693	AD	"	~0.74	"
1766	AD	"	~1.25	"
1845	AD	"	~0.63	"
1947	AD	"	~0.76	"
1970	AD	"	~0.2	Thorarinsson & Sigvaldason, 1972
1980	AD	"	~0.15	Mod. after Gronvold *et al.* 1983
1991	AD	"	~0.15	Gudmundsson *et al.* 1992
2000	AD	"	0.22	A. Höskuldsson *et al.* in press

Estimated dense rock equivalent volumes of known Hekla eruptions. HX are about 15 tephra layers of intermediate compositions, and volumes an order of magnitude less than H4 and H3. According to ongoing mapping, some older layers of this size are also found (B. Robertsdottir, pers. comm). Most of the volumes older than AD 1845 are very rough estimates. DRE – dense-rock equivalents.

The present work aims to define and account for the compositional variation within the two largest explosive eruptions of Hekla, H4 and H3. These two eruptions were selected because almost the whole range of magma compositions from Hekla is represented. The aim is to use these eruptions to construct a model of the Hekla magma system and outline the processes that take place during the evolution of silicic magma.

2. Geological setting

Hekla is located at the western margin of a propagating rift (Fig. 1) that extends southward from the eastern rift zone in Iceland (Oskarsson, Sigvaldason & Steinthorsson, 1982; Gudmundsson *et al.* 1992). The volcano forms a ridge, rising approximately 1000 m above the surrounding lava plateau, to about 1500 m above sea level. The Hekla ridge is superimposed on a cluster of basaltic Pleistocene hyaloclastite ridges that make up the western flank of the volcano and form a low mountain range to the west, parallel with the Hekla ridge. Eruptions of evolved magma occur on a 5 km long fissure along the spine of the Hekla ridge, and on short fissures on its flanks (Fig. 2). Basaltic, effusive eruptions occur on a fissure system parallel to the ridge. All the late Pleistocene hyaloclastite formations analysed in the Hekla region are basaltic (Fig. 2). Lava flows, most widespread south of the mountain, are of similar composition. Because they are covered by younger lava flows in the vicinity of Hekla, their origin cannot be traced, but topographic relations and chemical similarities of the ridges and the lavas indicate that the productive basaltic volcanism of the basement surrounding Hekla continued a few thousand years into the Holocene.

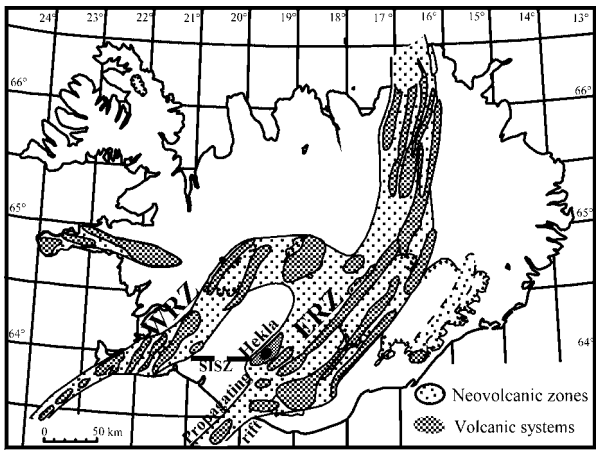

Figures 1. Volcanic zones of Iceland. The figure outlines the neovolcanic Quaternary formations of Iceland. WRZ denotes the Western Rift Zone of Iceland, and ERZ denotes the Eastern Rift Zone. SISZ is the South Icelandic Seismic Zone. Hekla is shown on the western margin of a propagating rift that extends south to the offshore Vestmannaeyjar volcanic centre. Volcanism on the propagating rift can be traced back to early Quaternary times. Rock suites of the propagating rift, which are alkalic to the south, and tholeiitic with alkalic affinities at the north termination, rest discordantly on older tholeiitic crust.

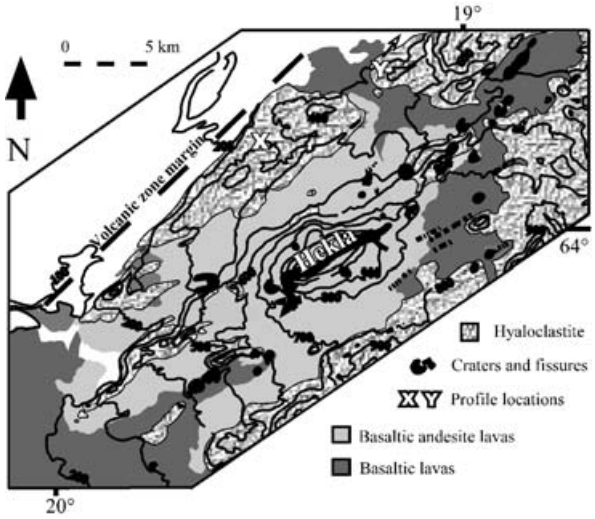

Figure 2. Geological outlines of the Hekla volcanic ridge. Evolved activity of Hekla is mostly confined to a fissure that extends about 5 km along the volcanic ridge. Most of the basaltic andesites originate in the fissure, and H4 and H3 deposits were erupted within the central segment of this fissure. Craters and fissures to the north and south of Hekla are mostly basaltic. The location of the H3 tephra profile is shown by X, and Y with arrow indicates the profile location of H4 20 km NE of the edge of the map.

The earliest activity of Hekla as an evolved volcanic centre (erupting basaltic andesite to rhyolite) probably occurred during early Holocene time. The first recorded silicic eruption from Hekla, H5, occurred roughly 7000 years ago. During the early Holocene, infrequent rhyolitic to dacitic Plinian eruptions dominated. No intermediate lavas are known from this early Holocene phase of volcanism, and rock fragments found in the H5 deposit are exclusively basaltic. However, xenoliths of basaltic andesite composition are abundant in the H4 deposit, which indicates that the first significant basaltic andesite production in the Hekla system followed the H5 eruption.

H4 was erupted 3826 ^{14}C years ago (Dugmore *et al.* 1995), or 4178–4202 years BP (Stuiver *et al.* 1998). The dense-rock equivalent (DRE) volume of the airfall deposit is estimated at 1.8 km^3 (Larsen & Thorarinsson, 1977). The deposit is compositionally graded from 56 to 72 % SiO_2. H3 is the most voluminous Hekla fallout, erupted 2879 ^{14}C years ago (Dugmore *et al.* 1995), or 2950–3041 years BP (Stuiver *et al.* 1998). The dense-rock volume is estimated at 2.2 km^3 (Larsen & Thorarinsson, 1977). The deposit is compositionally graded from 56 to 70 % SiO_2.

Data from other Hekla eruptions are included in this study for comparative purposes only; H5, the first known major explosive eruption of Hekla, is at least 0.7 km^3 dense-rock equivalent volume (Larsen & Thorarinsson, 1977), with composition ranging from 65 to 75 % SiO_2; new analyses from four other eruptions were done, from AD 1766, 1845, 1947 and 1970. The first three range from 63 to 54 % SiO_2, whereas the last one has a uniform composition of 54–55 % SiO_2.

3. Results

3.a. Sampling and analytical methods

Samples were selected to represent the compositional variation within each eruption. Samples were collected from tephra layers, and if available, from lava flows as well. The samples from H4 and H3 were collected by Gudrun Larsen. Samples from H5 were collected by Gudrun Larsen and Karl Ingolfsson, and sampled at equal intervals through the unstratified layer. Samples from other Hekla products analysed for comparison were collected by Gudrun Larsen and colleagues, from tephra layers and their respective lava flows. All samples were fresh and unaltered.

Samples of H4 tephra were collected from a 0.7 m thick profile at Sigalda, 30 km NE of Hekla. The sampling was done on the basis of colour gradation, and bulk samples were collected systematically through the Plinian deposit, each representing a 3 to 6 cm thick horizon. All samples consist of the largest pumice fragments from each bulk sample. The top of the deposit was somewhat eroded, so that the topmost sample probably does not represent the end of the explosive eruption. Sample H4-1 represents the first erupted material, but H4-12 represents the last erupted material available. No abrupt interface is seen between colour classes, but as the gradation is a distinctive feature of these deposits, they are regarded as 'zoned' deposits. H3 was sampled at Ófærugil, 8.5 km NW of Hekla, in a 5 m thick complete section close to the axis of maximum thickness of the Plinian deposit. Division into zones was made on the basis of colours, which changed more moderately than in H4. Samples consist either of pieces of pumice collected from 10 cm horizons, or of fragments of larger pumice clasts. H3-1 and H3-13 represent the assumed first and last erupted material, respectively.

Whole-rock major element composition was determined by the author, by combined wet chemical and XRF techniques at the geochemical laboratory of the Nordic Volcanological Institute. X-ray analyses of major oxides were performed using the method of Norris & Chappell (1977), and the alkalis and Mg by AAS after acid solution of the rocks. Trace element analyses were carried out on the same samples at the U.S. Geological Survey, Reston, VA. This part of the analytical work was done by Susan L. Russell-Robinson. Most of the trace elements were analysed by the INAA technique. The procedure is described in Roelands (1977). Cu, Ni, Cd and Pb were determined by ICP-AES, Mo and Nb by spectrophotometry, and B by emission spectroscopy. Samples from H5 were analysed by ICP-AES at the Nordic Volcanological Institute, by

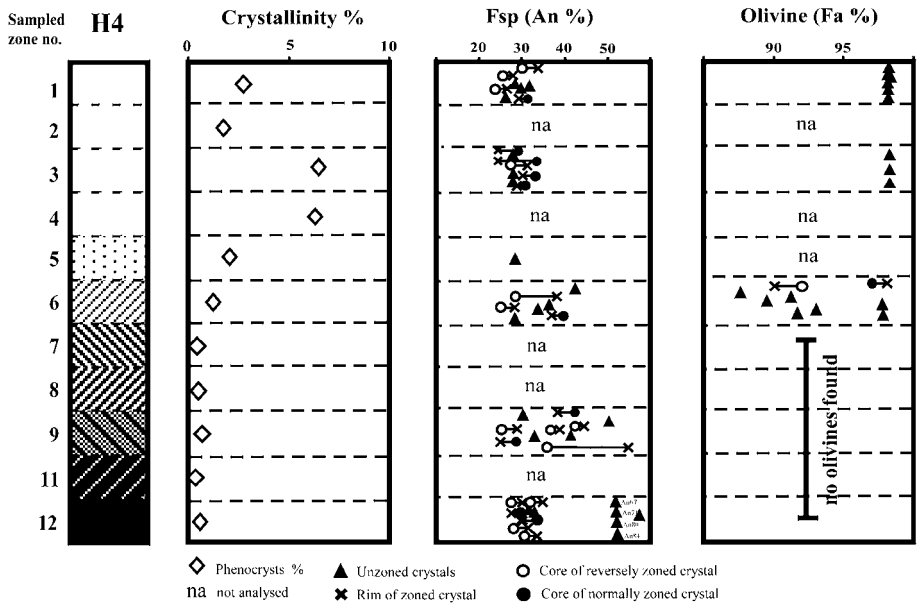

Figure 3. Crystallinity profile and composition of the most common phenocrysts in the H4 tephra layer. The layer is shown schematically as reversed stratigraphy in order to represent the conditions in the magma chamber, and colour changes are indicated by hatching as follows: zones 1–4 – white; zone 5 – yellowish white; zones 6–8 – greyish yellow or greyish pink; zones 9–12 – greyish brown to dark brown. Sample number 10 was not used in the research.

Niels Oskarsson. ICP analyses were performed on solutions of rock-powder fluxed with Li-metaborate and dissolved in 5 % nitric acid with 1.3 % hydrochloric and oxalic acids as described in Govindaraju & Mevelle (1987). Microprobe analyses of minerals were made on every other zone and microprobe glass analyses were made on a few zones for comparison with the whole rock compositions. Microprobe analyses were made on an electron microprobe (ARL-Q30) at the Nordic Volcanological Institute, using analytical conditions of 15 kV accelerating voltage, and 15–20 nA sample current for basaltic glass and minerals respectively, and a beam diameter of 2–3 μ. For silicic glasses, sample current was lowered to 10 nA in order to minimize Na-loss, and the samples moved under the beam for the same purpose.

3.b. H4 and H3 deposits

3.b.1. Zones and petrography

The existence of a magma chamber beneath Hekla has been assumed for a long time, based on geochemical characteristics, eruption mechanism, and ground deformation (Kjartansson & Gronvold, 1983; Soosalu & Einarsson, 2004). The Hekla rock suite is different from the tholeiitic basalt erupted from the adjoining fissure system as confirmed by isotopic evidence (Sigmarsson, Condomines & Fourcade, 1992), and compositions change systematically between eruptions. Petrological constraints suggest the pre-eruptive equilibrium depth of the Hekla 2000 magma was about 14 km (Hoskuldsson *et al.* in press). Several attempts have also been made to locate the chamber by geophysical methods. Kjartansson & Gronvold (1983) estimated the centre of deflation after the 1980 eruption at 8 km depth. Recent seismic evidence favours a depth of 14 km or more (Soosalu & Einarsson, 2004).

As a starting point of the present study, the different fallout zones were assumed to represent the relative positions of material in a magma chamber before eruption, practically undisturbed by eruption withdrawal (Blake & Fink, 1987). Accordingly, compositions are plotted against schematic reversed stratigraphic height in Figures 3, 4, 5 and 6. In the discussion of these deposits in the following chapters, 'upper' and 'lower' always refer to location in a hypothetical magma chamber, not to the respective tephra layers. Zonation of H4 is shown in Figure 3. Zones 1 to 5 consist of white to yellowish-white pumice. In these first five zones, some crystals, mainly feldspars, are visible in hand specimen. In the sixth zone, an abrupt change to greyish pumice is encountered, and no crystals are seen. Colour gradation is seen in most zones; the last one is almost black. No clear interface separates the zones. Zonation of H3 is shown in Figure 4. The first erupted pumice is not as white as in H4, but even more crystals are visible. Zones 1 to 4 display faint colour gradation from almost white to beige. Colour change in the H3 layer is continuous apart from pale streaks or bands in the dark-grey zone number 11. Grading through the deposit is more moderate, turning to black in the last zone. No distinct interfaces are seen. Pumice in zones 5 to 13 seems aphyric.

Whole-rock analyses of major and trace elements in the H4 fallout are listed in Table 2, and glass

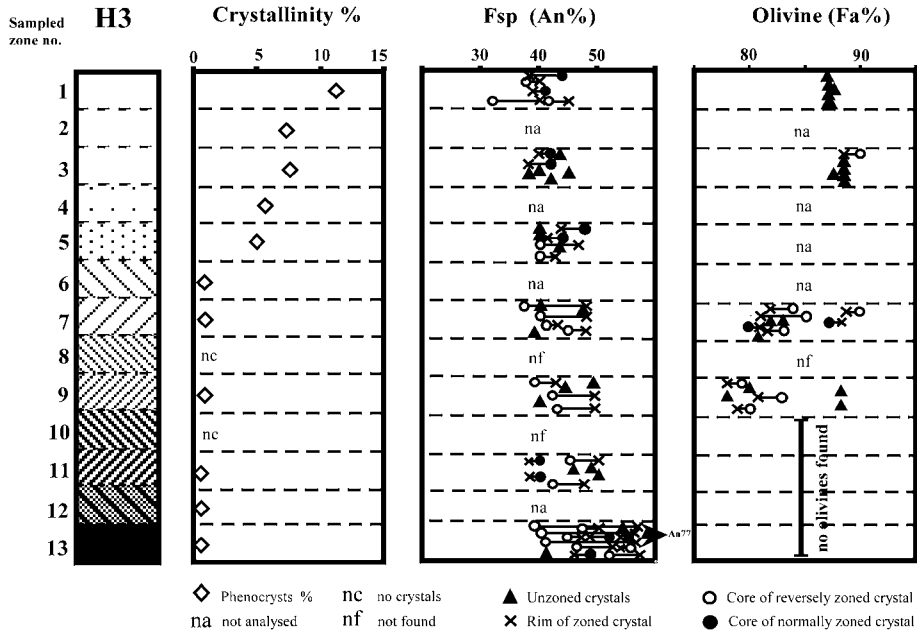

Figure 4. Crystallinity profile and composition of the most common phenocrysts in the H3 tephra layer. The layer is shown schematically as reversed stratigraphy and colour changes are indicated by hatching as follows: zones 1–4 – white to yellowish white; zones 5–9 – greyish yellow to greyish pink; zones 10–12 – dark brown to greyish brown; zone 13 – black.

compositions are given in Table 5. The respective analyses of the H-3 fallout are in Tables 3 and 5. Table 4 gives compositions of four young eruptions analysed for comparison, and Table 6 shows major and some trace element analyses of H5, also analysed for comparison.

3.b.2. Petrology and mineral composition

The crystal content of H4 is up to 7 % in zones 3 and 4, but is less than 1 % in zones 6 to 12 (Fig. 3). In H3 the most silicic zones 1 to 5 contain from 11 to 2 % crystals, but zones 5 to 13 less than 1 % (Fig. 4). In both deposits plagioclase, olivine, clinopyroxene, magnetite and occasional ilmenite are present as phenocrysts, plagioclase being the most abundant. Tiny grains of zircon are found as an accessory mineral within plagioclase crystals in most zones of both layers. All phenocrysts are small; the plagioclase ranges up to 1 mm, but the others are smaller than 0.5 mm. The zircon crystals are of micrometre scale.

The composition of plagioclase and olivine in the two deposits H4 and H3 is outlined in Figures 3 and 4. The compositions of plagioclase in the most silicic parts of the layers are fairly uniform. In H4 it ranges from An24 to An34 and in H3 from An38 to An45. The olivine composition is also uniform, Fa97 in H4 and Fa87 in H3. These compositions are consistent with the respective whole rock and glass compositions and indicate equilibrium conditions. In the less evolved, less crystallized zones of the deposits, the compositional range increases for both minerals, with reversed zoning dominating throughout the sequence. Cores of the most sodic plagioclases, of about An25 in H4 and An40 in H3, occur through the sequence. In this more basaltic part of H4, olivine was only found in zone 6, showing a range of composition from Fa87 to Fa97, and in H3 in zones 7 and 9, showing compositional range of Fa77 to Fa89. The zoning of the olivines is mostly reverse.

3.b.3. Geochemistry

Several major element sections through both deposits, H4 and H3, are shown in Figure 5. Glass compositions are indicated by arrows for some elements if different from whole rock compositions. Trace element concentrations are plotted in Figure 6. For comparison, Zr content in samples from the H5 eruption is also plotted in the same figure.

The most outstanding feature of H4 is a compositional break at the boundary between zones H4-5 and H4-6, where the silica content drops from 71 % to 65 % (Fig. 5). This break is also reflected in most elements, and follows a decrease in crystal content between zones 5 and 6. The change in composition of the plagioclase from homogeneous An25 to reverse zoning occurs at a similar level (Fig. 3). As chemical analyses of minerals were only done in every other zone, the location of a compositional break was confirmed by microscopic features. In zones 1 to 5, the concentrations of major elements remain virtually constant, whereas in zones 6 to 12 they show considerable gradation. A slight difference in whole-rock and glass composition reflects crystallization in the most silicic part of both layers. No significant difference is seen in the darker, less crystallized part. Light bands, only seen in zone 6 in H4 and zone 11 in H3, have the composition of the most silicic material in the respective layer. An

Table 2. The H4 tephra

Zones	1	2	3	4	5	6	7	8	9	11	12
SiO_2	71.74	72.36	72.14	71.74	71.34	65.25	64.09	62.87	61.61	57.82	56.99
TiO_2	0.20	0.16	0.17	0.17	0.21	0.47	0.55	0.70	0.79	1.27	1.50
Al_2O_3	12.87	13.12	13.00	13.06	13.04	14.16	14.31	14.30	14.16	14.69	14.58
Fe_2O_3	–	0.38	0.34	0.48	0.45	1.05	1.46	1.93	2.14	2.32	3.55
FeO	–	1.81	1.79	1.80	2.42	5.67	6.20	7.22	7.47	8.17	7.50
MnO	–	0.08	0.08	0.09	0.11	0.22	0.23	0.25	0.25	0.23	0.24
MgO	–	0.06	0.07	0.08	0.08	0.14	0.33	0.57	0.98	1.88	2.05
CaO	1.49	1.48	1.48	1.50	1.78	3.42	3.67	4.18	4.37	5.18	5.68
Na_2O	–	4.73	4.71	4.78	4.85	4.80	4.78	4.58	4.71	4.07	3.84
K_2O	2.81	2.81	2.77	2.80	2.69	2.01	1.91	1.74	1.66	1.39	1.31
P_2O_5	0.00	0.00	0.00	0.00	0.02	0.07	0.12	0.19	0.25	0.52	0.62
H_2O	2.28	2.16	2.97	2.69	2.53	1.24	1.16	0.90	0.65	0.74	0.92
Cl	680	660	680	580	520	400	360	320	320	290	260
F	1600	1480	1360	1360	1320	1120	960	920	880	1040	880
B	6.1	4.6	5.3	16	5.2	4.2	3.6	3.5	3.3	2.4	3.6
Rb	63	63	58	61	64	49	52	44	51	39	36
Cs	0.9	0.8	0.8	0.8	0.7	1.2	1.1	0.7	<2.0	0.5	0.6
Ba	699	701	635	622	588	591	484	458	474	390	360
Zr	394	394	425	270	460	1000	1150	1390	1410	645	620
Hf	11.5	11.4	11	11	13.2	23.7	24.9	28.4	27	13.6	12.4
Nb	80	78	79	78	79	74	73	63	67	56	53
Ta	6.27	5.89	5.67	5.61	5.64	4.8	4.79	4.38	4.06	3.74	3.88
Pb	7	4.3	5.7	6.8	9.4	5.4	4.4	6	2.6	4	3.4
Th	11.2	11.5	11	12.1	11	8.7	8.1	7.4	6.8	5.8	5.3
U	3.4	2.7	2.7	2.5	2.5	2.3	2.2	1.3	2.2	1.7	1.3
Sc	4.54	4.29	3.97	4.32	5.08	16.2	19.8	24.3	23.6	18	19
Cr	3.4	2.2	<8.0	<7.0	3.2	5.4	<20	<20	5.7	<10	5.4
Co	1.3	0.7	0.7	0.9	1.1	1.9	3	3.8	4	13	15
Ni	4	2	2	3	4	4	7	3	1	3	6
Cu	14	14	15	13	14	19	20	27	21	22	23
Zn	130	130	130	130	140	170	180	180	170	180	170
Mo	–	4.8	4.8	4.6	4.6	4.2	4.2	2	3.6	3	2.4
Cd	0.34	0.36	0.32	0.3	0.32	0.31	0.34	0.45	0.28	0.28	0.26
La	79	94	79	123	94	75	69	63	61	55	54
Ce	159	193	165	239	189	157	142	128	126	117	113
Nd	91	90	87	112	94	89	79	72	75	72	70
Sm	16.6	16.9	14.2	19	17.1	15.8	15.3	14.1	14.2	12.5	14.1
Eu	2.87	3.07	2.88	3.47	3.32	4.28	4.17	4.17	4.28	4.23	4.15
Gd	18.6	20.3	18.2	19.8	18.2	17.6	15.8	15.1	15.8	15.4	14.4
Tb	2.48	2.79	2.69	2.22	2.28	2.2	2.04	2.28	1.95	1.97	1.89
Tm	1.46	1.39	1.11	1.31	1.26	1.2	1.48	1.11	1.16	1.06	0.76
Yb	9	9.1	8.8	8.9	9.1	9.5	9.5	9	9	7.1	6.5
Lu	1.24	1.23	1.18	1.18	1.26	1.41	1.38	1.33	1.29	1	0.95

Chemical composition of the H4 tephra layer (whole rock analyses). Major element concentrations are given as weight % of the oxides; trace element concentrations are given in ppm.

outstanding change in H4 at the compositional break is a decrease in the content of residual volatiles and some trace elements, such as F, Cl and Th in zones 6 to 12, and significant enrichment in Zr, Sc (Fig. 6), Hf and Yb in zones 6 to 9. Exceptional enrichment of the trace elements Th and La is observed in zone 4 as discussed below (Fig. 6).

In H3 a break in chemical trends between zones 4 and 5 is much less pronounced than the compositional break in H4, but is visible for CaO, K_2O and FeO between zones 4 and 5 (Fig. 5). Changes in the crystal content and mineral composition occur at a similar level (Fig. 4). Zones H3-1 to 5 are lower in silica than the respective zones in H4, and the glass composition differs slightly from the whole-rock composition. In contrast to H4, the major element concentrations of H3 vary only moderately through zones 1 to 12. A gap associated with a colour change from greyish-brown to nearly black where the SiO_2 content drops from 63 % to 56 % separates zones 12 and 13, and is reflected in several elements (Figs 5, 6). H3-11 is the only zone in which the light bands could be analysed. Their glass composition is identical to the earliest erupted pumice (Table 5). Trace element concentrations vary only slightly through most of the H3 profile (Fig. 6). Most are similar to those of H4, except for lower halogens, Th and La concentrations, and only slight enrichment in Zr (Fig. 6). The Zr content of H5 increases abruptly below the level of 69 % SiO_2, showing a similar trend to H4, but with less enrichment (Fig. 6).

Chondrite-normalized REE patterns are shown for all zones in H4 and H3 on Figure 7a and Figure 7b, respectively. In H4, LREE enrichment increases from zone 1 to zone 4, and moderate Eu depletion occurs.

Table 3. The H3 tephra

Zones	1	2	3	4	5	6	7	8	9	10	11	12	13
SiO_2	67.82	68.46	69.31	68.69	66.96	67.68	66.48	66.26	65.10	63.55	62.49	62.71	56.15
TiO_2	0.35	0.33	0.34	0.33	0.39	0.41	0.43	0.46	0.51	0.70	0.76	0.69	1.70
Al_2O_3	14.42	14.12	14.55	14.28	14.57	14.87	14.65	14.78	14.88	14.92	15.24	15.01	14.73
Fe_2O_3	0.70	0.81	0.68	0.65	0.81	0.60	1.38	1.07	1.31	3.12	2.02	1.46	4.47
FeO	3.62	3.52	3.73	3.55	4.41	4.97	4.56	4.87	5.22	5.00	6.48	6.50	7.34
MnO	0.13	0.13	0.14	0.13	0.16	0.17	0.18	0.18	0.18	0.21	0.21	0.21	0.24
MgO	0.27	0.19	0.24	0.21	0.33	0.30	0.36	0.37	0.47	0.91	0.98	0.85	2.30
CaO	2.59	2.48	2.59	2.46	3.08	3.20	3.27	3.29	3.59	4.13	4.36	4.07	6.09
Na_2O	4.66	4.83	4.93	4.89	4.90	4.88	4.82	4.83	4.83	4.88	4.69	4.66	3.96
K_2O	2.28	2.31	2.35	2.30	2.09	2.13	2.07	2.05	1.99	1.75	1.74	1.75	1.27
P_2O_5	0.05	0.04	0.06	0.03	0.08	0.07	0.10	0.09	0.11	0.22	0.14	0.19	0.81
H_2O	1.94	1.63	1.15	1.68	0.99	0.94	1.08	0.96	1.16	0.73	0.42	0.72	0.75
Cl	400	400	450	400	380	350	370	390	370	340	280	310	260
F	1040	1080	1120	1080	1000	1000	1360	1040	1040	960	960	960	1000
B	4.4	3.3	4.2	4.5	4.4	4.8	4.8	5	4.1	3.4	4	3.9	2.6
Rb	60	51	55	58	48	48	51	51	49	44	47	48	36
Cs	0.8	0.7	0.8	0.8	0.7	0.9	0.5	0.5	0.7	0.8	0.6	0.7	0.8
Ba	602	609	612	603	563	651	569	588	523	545	491	533	427
Zr	591	690	649	748	822	758	864	803	747	726	630	524	420
Hf	14.4	15.8	14.5	15	17.5	17.6	17.7	17.3	16	14.6	14.2	14.4	10.7
Nb	64	65	67	65	66	67	66	66	63	55	53	57	53
Ta	4.98	4.93	4.99	5.22	5.19	5.06	5.1	4.99	4.63	4.71	4.59	4.58	4.3
Pb	<1.0	<1.0	<1.0	4	<1.0	4.6	<1.0	5	<1.0	4	7	2	5.4
Th	9.4	9.6	9.5	9.6	9	8.9	8.8	8.5	8.1	7.7	7.4	7.5	5.4
U	2.9	2.9	2.9	2.9	2.8	3.1	2.7	2.6	2.5	2.7	2.6	2.4	1.8
Sc	9.24	9.17	9.27	8.8	11.7	12.1	12.2	12.3	12.9	14.6	15.2	14.3	18.8
Cr	<9.0	<10.0	3.6	<10.0	<9.0	<20.0	<20.0	<20.0	<10.0	<20.0	5.4	<10.0	<20.0
Co	2.6	2.4	2	1.9	1.9	2.2	2.6	2.9	3.4	5	4.9	5	17
Ni	<1	<1	2	<1	3	<1	<1	2	<1	5	<1	<1	9
Cu	20	16	17	14	18	17	17	19	17	19	21	19	26
Zn	120	120	120	120	140	140	150	160	160	160	150	150	180
Mo	4	–	4.4	4.4	4	4.1	4.2	4.4	4	3.8	3.2	–	3
Cd	0.19	0.19	0.23	0.18	0.21	0.17	0.2	0.16	0.2	0.13	0.15	0.08	0.06
La	72	73	73	73	69	68	68	66	64	60	59	60	53
Ce	148	151	143	149	141	142	140	136	130	123	121	122	111
Nd	85	83	79	84	80	81	80	74	69	71	77	70	74
Sm	15.8	14.2	15.4	16	15.3	16	15.3	13.1	14.6	14.3	13.2	14.4	14.1
Eu	3.54	3.5	3.32	3.55	3.69	3.82	3.55	3.6	3.62	3.75	3.8	3.74	4.21
Gd	15.6	18.5	19.4	16.6	16.6	17.2	15.9	15.8	14.3	15.2	16.2	14	15.6
Tb	2	2.05	2.26	2.26	2.23	2.13	2.17	2.18	2.1	2.2	2.25	2.18	2.21
Tm	1.33	1.36	1.33	1.42	1.36	1.44	1.54	1.36	1.25	1.24	1.23	1.1	1.1
Yb	8.3	8.6	8.2	8.2	8.3	8.4	8.4	8.1	7.5	7.3	7.2	7.3	6.6
Lu	1.16	1.19	1.17	1.18	1.18	1.19	1.17	1.15	1.11	1.04	1.04	1.06	0.93

Chemical composition of the H3 tephra layer (whole rock analyses). Major element concentrations are given as weight % of the oxides; trace element concentrations are given in ppm.

Zones 6 to 12 display less LREE enrichment and no Eu anomaly, and zones 11 and 12 are HREE-depleted. The REE patterns for H3 are more moderate and gradual through the zones. Zone 3 shows the most evolved composition; LREE enrichment is not as prominent and diminishes continously from zone 3 to zone 13. The same patterns are shown for the faint Eu-anomaly and HREE depletion. All chemical gradations through the layers are more moderate in H3 than H4.

4. Discussion

4.a. Evidence from mineralogy

The mineralogical characteristics described in the preceding section provide the strongest clues by far to the processes responsible for the chemical gradation of the large Hekla layers. The most silicic part of the layers contain 2 to 11 % crystals, mostly plagioclase and some fayalitic olivine. In H4, crystallinity is highest in zones 3 and 4, about 7 %, but in H3, zone 1 has the highest crystallinity, 11 % (Figs 3, 4). The mineral composition is fairly uniform, and apparently crystal nucleation has occurred in conditions close to equilibrium.

It was shown on the basis of Th isotopes (Sigmarsson *et al.* 1991; Sigmarsson, Condomines & Fourcade, 1992), that the silicic Hekla magma is neither related to the basaltic andesites nor the basalts of the volcanic system. Therefore, production of the silicic magma by crystal fractionation of the basaltic andesite can be ruled out. As the feldspars plot close to the eutectic in the Ab–Or–Qz diagram, and equilibrium conditions are indicated by homogeneous crystal composition, it is strongly suggested that the silicic magma is produced by partial melting of the local crust. Segregation and

Table 4. Four Hekla eruptions from the last 250 year period

Samples	H1766-T	H1766-L	H1845-T	H1845-L	H1947-T	H1947-L	H1970-T	H1970-L
SiO_2	58.99	54.35	59.70	54.80	61.55	56.13	54.90	54.36
TiO_2	1.30	1.96	1.17	1.88	0.98	1.75	1.89	2.05
Al_2O_3	15.20	14.50	15.20	14.66	15.36	14.54	14.61	14.64
Fe_2O_3	1.88	1.74	1.72	1.23	0.74	2.08	4.15	2.64
FeO	8.13	10.42	7.39	10.54	7.67	9.25	7.32	9.70
MnO	0.23	0.25	0.22	0.25	0.21	0.24	0.25	0.25
MgO	1.50	2.73	1.77	2.97	1.42	2.75	2.76	3.03
CaO	5.42	6.68	5.06	6.53	4.58	6.29	6.56	6.89
Na_2O	4.41	4.20	4.52	4.20	4.74	4.27	4.17	4.15
K_2O	1.54	1.26	1.60	1.31	1.72	1.31	1.28	1.23
P_2O_5	0.54	0.97	0.41	0.94	0.32	0.83	0.79	1.03
H_2O	0.00	0.35	0.00	0.32	0.13	0.17	0.32	–
Cl	340	330	370	420	380	320	320	460
F	1160	1600	1000	1120	1040	920	1120	1360
B	2.1	2.1	1.9	1.7	3.9	2.7	2.6	2.1
Rb	35	35	38	32	40	36	36	34
Cs	<1.0	0.4	0.5	0.4	0.7	0.8	<2.0	<1.0
Ba	429	417	426	377	469	418	384	388
Zr	320	490	500	320	604	470	410	500
Hf	13.1	11.5	12.3	11.2	13.4	11.2	10.9	10.6
Nb	68	63	64	64	70	66	67	68
Ta	4.64	4.5	4.29	4.26	4.85	4.6	6.56	6.35
Pb	2.4	3.2	3.2	3.4	2.8	3	1.3	3.2
Th	5.7	4.9	5.9	5	6.7	5.2	4.9	4.7
U	1.5	1.8	1.2	1.4	2.1	2	2	1.6
Sc	18.5	21.6	16.6	20.6	16.1	19.65	21.1	21.3
Cr	<20.0	<20.0	<20.0	<20.0	<20.0	<20.0	7.4	<20.0
Co	12	20	11	18	8	14	36	23
Ni	2	2	4	1	4	7	26	9
Cu	11	11	18	10	15	12	17	8
Zn	190	210	180	200	180	200	200	200
Mo	–	2.6	–	2.9	3.4	2.9	–	–
Cd	0.21	0.17	0.34	0.15	0.33	0.23	0.25	0.39
La	56	54	56	50	59	53	52	52
Ce	128	124	118	121	125	121	114	113
Nd	76	80	66	80	75	80	71	73
Sm	12.4	13.8	11.7	12.2	12.8	13	12.6	13.1
Eu	4.71	4.91	4.21	4.71	4.3	4.74	4.59	4.54
Gd	18.3	17	14.8	15.5	14.3	15	17	14.9
Tb	2.3	2.44	2.03	1.92	2.16	2.13	2.05	2.33
Tm	1.08	1.06	0.97	0.87	1.02	1.09	0.83	1
Yb	7.1	7	6.8	6.7	7.3	6.6	6.6	6.5
Lu	1.01	1	0.95	0.94	1.03	0.95	0.91	0.91

Chemical composition of products from four young Hekla eruptions (whole rock analyses). T denotes tephra sample. L denotes lava sample. Major element concentrations are given as weight % of the oxides; trace elements are given in ppm.

displacement of magma near its source into a space created by crustal spreading is favoured (Gunnarsson, Marsh & Taylor, 1998). Since a silicic melt produced by anatexis is inevitably close to equilibrium with several mineral phases, crystal nucleation is favoured through the entire magma body. As silicic magma is the first erupted part of each eruption and this magma is followed by less evolved, sparsely crystallized magma, crystallization was probably enhanced near the (cooler) roof of the magma chamber. Crystallization has little effect on the major element chemistry of near-eutectic melts. Accordingly, the silica range in the uppermost zones of the chamber is only 1.04 % and 2.35 % in H4 and H3, respectively.

In the dacitic to basaltic andesitic part of the deposits, where the crystal content is less than 1 % in most zones, the disequilibrium mineral composition reveals the hybrid character of the magma in the deeper part of the reservoir. Reverse zoning of most plagioclase crystals provides supporting evidence for mixing of two magmas. Crystals are of similar size as in the silicic part, but in some zones no crystals were found. The main mineralogical indicator for magma mixing is the ubiquitous occurrence of cores of sodic plagioclase through the sections, reversely zoned to equilibrium with the glass composition of each layer. Resorption of minerals is more common as the hybrid magma becomes more mafic. These outstanding disequilibrium characteristics all indicate mixing of the evolving silicic magma with a basaltic magma intruded from below. Similar reversed zoning has indeed been observed in the intermediate rocks of the Krafla volcanic centre, where mixing between rhyolite and tholeiitic basalt was suggested (Jonasson, 1994).

Accessory phases have been suggested as indicators of magma chamber processes (Robinson, Miller &

Table 5. H4 and H3, glass compositions

Zone / no. of shards	SiO_2	TiO_2	Al_2O_3	FeO	MnO	MgO	CaO	Na_2O	K_2O	P_2O_5	Total
H4-1 / 6	73.60	0.09	13.10	1.90	0.10	0.00	1.41	4.94	2.76	0.00	97.90
Std dev.	2.03	0.07	0.18	0.08	0.06	0.00	0.08	0.24	0.10	0.00	
H4-3 / 8	73.61	0.07	12.71	1.93	0.11	0.02	1.60	4.64	2.74	0.00	97.43
Std dev.	0.77	0.06	0.39	0.17	0.06	0.02	0.23	0.29	0.08	0.00	
H4-6 Lb / 3	72.43	0.09	12.78	1.72	0.06	0.08	1.14	4.46	2.77	0.33	95.86
Std dev.	0.64	0.03	0.09	0.09	0.05	0.05	0.23	0.39	0.03	0.15	
H4-6 / 5	66.50	0.45	14.15	6.05	0.32	0.20	3.55	4.47	1.94	0.17	97.80
Std dev.	0.97	0.17	0.20	0.52	0.12	0.05	0.25	0.55	0.12	0.11	
H4-9 / 10	61.22	0.79	14.72	9.60	0.30	0.84	4.70	4.59	1.54	0.30	98.60
Std dev.	0.61	0.06	0.26	0.42	0.07	0.11	0.33	0.26	0.16	0.11	
H4-12 / 4	58.32	1.44	14.63	9.70	0.30	2.02	5.73	3.94	1.28	0.71	98.07
Std dev.	1.05	0.07	0.67	0.29	0.07	0.22	0.22	0.15	0.12	0.12	
H3-1 / 6	71.86	0.16	13.58	2.88	0.17	0.12	1.95	4.43	2.49	0.02	97.66
Std dev.	0.54	0.06	0.52	0.22	0.06	0.01	0.14	0.25	0.15	0.03	
H3-3 / 5	71.80	0.23	13.70	2.93	0.10	0.14	2.15	5.18	2.50	0.00	98.73
Std dev.	0.58	0.00	0.32	0.21	0.08	0.08	0.14	0.29	0.05	0.00	
H3-7 / 8	68.24	0.49	14.74	5.46	0.19	0.33	3.65	4.03	1.95	0.07	99.15
Std dev.	0.78	0.09	0.24	0.27	0.07	0.10	0.28	0.48	0.04	0.08	
H3-9 / 8	65.92	0.47	14.89	6.36	0.21	0.59	3.61	4.50	1.89	0.15	98.59
Std dev.	0.74	0.11	0.31	0.25	0.06	0.10	0.31	0.33	0.04	0.05	
H3-11 Lb / 4	71.23	0.15	13.37	3.67	0.13	0.11	1.56	4.22	2.56	0.06	97.06
Std dev.	0.27	0.06	0.73	0.56	0.06	0.01	0.10	0.27	0.13	0.06	
H3-11 / 4	61.36	0.76	14.90	7.71	0.26	0.75	4.59	5.03	1.44	0.24	97.04
Std dev.	1.20	0.15	0.17	0.54	0.07	0.19	0.13	0.23	0.20	0.10	
H3-13 / 7	57.79	1.78	14.41	10.97	0.28	2.01	6.22	3.79	1.32	0.87	99.44
Std dev.	0.37	0.17	0.23	0.30	0.06	0.28	0.23	0.29	0.09	0.09	

Representative microprobe glass analyses (wt %). Lb = light bands in the pumice. Each analysis represents the average of several shards.

Table 6. The H5 tephra

Sample	2	3	4	5	7	8	9	10	11	12	13	14	15
SiO_2	72.52	73.03	74.30	75.01	74.17	69.58	69.53	73.43	73.10	68.73	67.84	65.40	66.73
TiO_2	0.41	0.40	0.21	0.18	0.24	0.89	0.85	0.42	0.38	0.46	0.49	0.59	0.54
Al_2O_3	13.98	13.90	13.72	13.33	14.02	13.81	13.72	13.24	13.34	14.35	14.37	15.44	14.37
FeO	3.30	3.16	2.49	2.24	2.41	4.95	4.63	2.99	2.99	5.55	5.51	6.88	6.74
MnO	0.09	0.10	0.08	0.08	0.08	0.10	0.11	0.09	0.09	0.16	0.17	0.20	0.20
CaO	2.21	2.15	1.83	1.78	1.78	2.72	3.04	2.08	2.12	3.16	3.41	3.75	3.38
MgO	0.37	0.42	0.16	0.12	0.15	0.98	0.90	0.33	0.30	0.35	0.36	0.51	0.50
Na_2O	4.33	4.02	4.39	4.28	4.56	4.04	4.27	4.32	4.46	4.36	4.98	4.35	4.63
K_2O	2.58	2.63	2.65	2.83	2.43	2.65	2.69	2.88	3.01	2.54	2.53	2.44	2.52
P_2O_5	0.08	0.07	0.04	0.03	0.04	0.15	0.14	0.09	0.09	0.16	0.17	0.25	0.22
Ba	643	601	635	646	724	617	596	622	628	536	502	538	501
Co	6.3	7.6	16.4	1.3	2.7	18.1	17.9	4.8	5.6	3.3	15.2	4.9	8.5
Cr	9.6	6.2	6.3	7.2	4.2	14.7	14.3	6.7	7.6	6.8	7.0	5.1	5.7
Cu	30.7	22.3	14.9	12.9	14.4	39.2	33.0	15.5	15.7	16.6	18.7	22.5	18.0
Ni	14.2	12.7	9.7	6.7	9.5	16.4	12.8	7.6	8.6	1.9	3.8	4.9	4.3
Sc	7.2	7.1	5.9	5.6	5.8	11.6	10.8	7.2	7.3	13.1	12.8	14.7	13.2
Sr	145	136	125	127	136	163	167	149	147	216	213	222	205
V	14.5	21.2	3.3	2.1	1.7	68.5	66.1	15.6	12.2	5.7	6.5	14.7	10.0
Y	86	81	88	88	93	78	75	79	80	90	86	87	81
Zn	111	105	101	100	91	115	110	111	110	146	145	152	138
Zr	288	268	262	260	282	230	249	299	314	833	842	887	837

Chemical composition of the H5 tephra layer (whole rock analyses). Major element concentrations are given as weight % of the oxides; trace element concentrations in ppm.

Ayers, 1997; Gunnarsson, Marsh & Taylor, 1998). A chemical fingerprint of an accessory phase most pronounced in the fourth uppermost zone in H4, although not confirmed by mineralogy, is high enrichment of the light REE and Th. This is distinctive in the chondrite normalized plot (Fig. 7) and in Figure 6. Therefore, small-scale accumulation of the accessory mineral allanite is suggested, since distribution coefficients for La, Ce, Nd, Sm, Gd and Th in allanite are very high, and hence can account for the enrichment (Henderson, 1984; Hildreth, 1979, 1981). This is more decisive as the Th enrichment is not compatible with a Zr anomaly (Fig. 6). Taking such phases into account without mineralogical confirmation was also found necessary by Furman, Frey & Meyer (1992), in their study on the evolution of Icelandic central volcanoes.

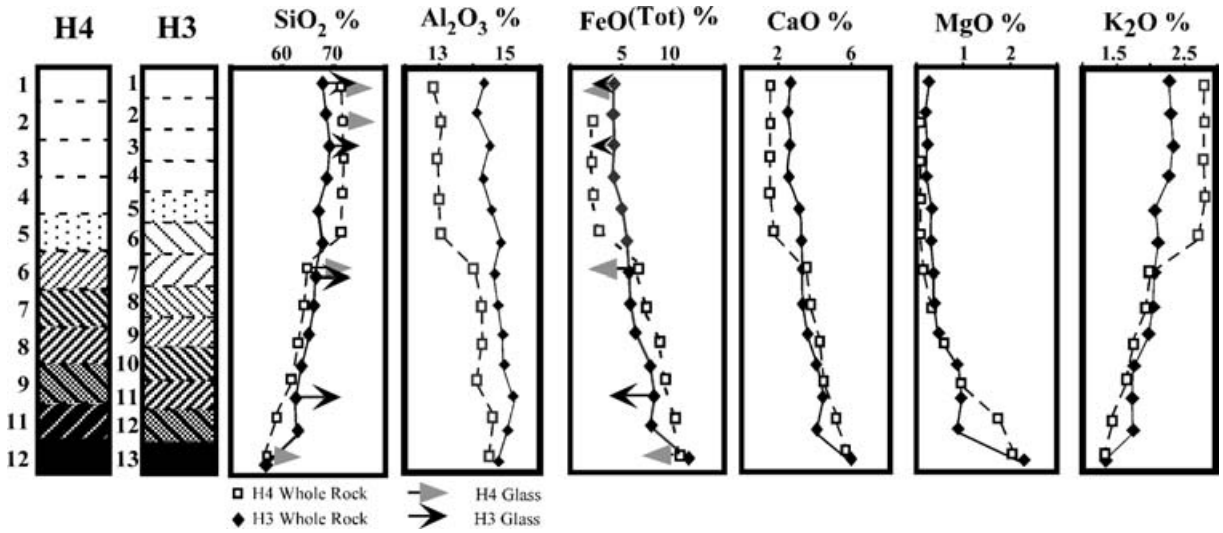

Figure 5. Major element variation in H4 and H3 deposits shown as reversed stratigraphy. Glass compositions are only shown if different from whole-rock composition of the corresponding zone. In some cases, two glass compositions were found in the same zone, as discussed in the text.

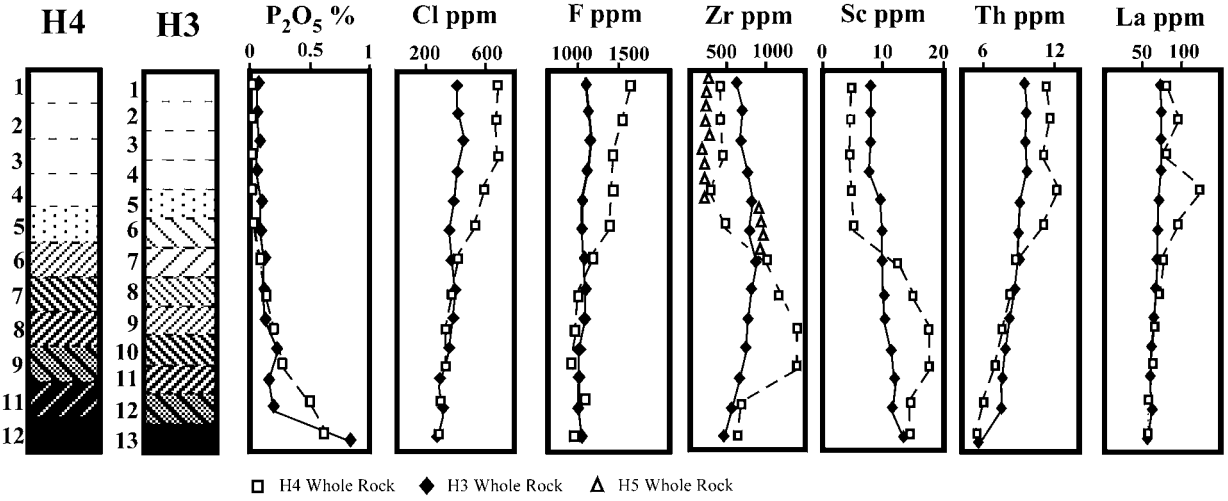

Figure 6. Trace element variation in H4 and H3 ash layers shown as reversed stratigraphy (ppm). Zr content in H5 is shown for comparison at similar stratification levels as in H4 and H3. Although no visible zonation, the layer was sampled in several steps from bottom to top. No basaltic andesite compositions were found.

In H4, anomalous enrichment of Zr, Hf, Sc and Yb in the four zones 6 to 9 below the crystallizing zones can only be explained by settling of plagioclase crystals with zircon embedded within them, as very small zircon grains were found as inclusions in plagioclase in zones H4-2 to H4-9, and in zones 1 to 11 in H3. The Zr enrichment is plotted against SiO_2 on Figure 8 for all zones of H4 and H3. For H5 only Zr is plotted on the figure. Figure 8 also shows the elements Hf, Sc and Yb in H4 and H3. The crystal chemistry of zircon allows Hf to incorporate by simple substitution, but Sc and Yb substitute by a coupled mechanism (Hoskin & Schaltegger, 2003). Liquidus temperatures calculated by the MELTS program (Ghiorso & Sack, 1995), and M-value as presented by Hanchar & Watson (2003), were used to evaluate the zircon saturation of the samples. These zircons could only have been captured by mixing from the silicic magma which is saturated in zircon. The hybrid magma is strongly undersaturated in zircon, hence the zircon crystals could not have formed in that magma.

The pronounced negative Eu anomaly seen in the silicic part almost disappears in zone 6 (Fig. 7a). This change in Eu is attributed to plagioclase settling, and possibly dissolution of the smaller crystal population upon mixing. The zircon-enriched feldspar began to settle since the plagioclase phenocrysts are heavier than the silicic melt (s.g. 2.6 v. 2.2), according to calculations done with the MELTS program (Ghiorso & Sack, 1995). It has been suggested that static conditions allow mineral settling, based on density difference alone (Sparks, Huppert & Turner, 1984). According to

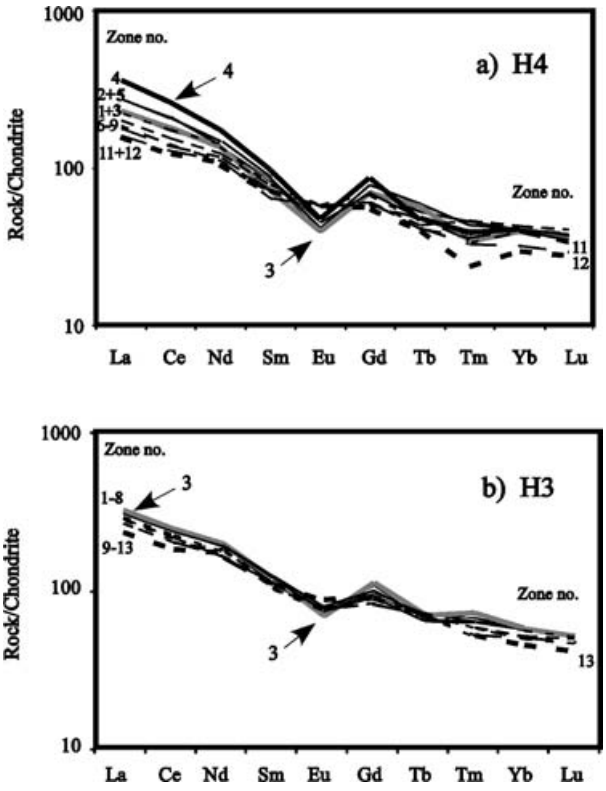

Figure 7. (a, b) Chondrite-normalized REE-concentrations for the whole rock analyses of (a) H4. Zones 1, 2, 4 and 5 are shown by whole lines, zone 3 by grey solid line, and zones 6–12 by dashed lines. Arrows indicate which zone is the most Eu-depleted (zone 3), and the most LREE-enriched (zone 4). (b) H3. Zones 1, 2, 4, 5, 6, 7 and 8 are shown by solid lines, zone 3 by grey solid line, and zones 9–13 by dashed lines. Arrows indicate the zones which are the most Eu-depleted (zone 3), and the most LREE-enriched (zone 3).

ion probe analyses of melt inclusions in plagioclase in H3 (Niels Oskarsson, pers. comm.), the Hekla magmas contain about 5 % H_2O. Viscosity of the H4 silicic melt was calculated by MELTS about $10^{4.5}$ Pa·s at 5 % H_2O.

4.b. Chemistry of mixing

In accordance with the chemical and mineralogical characteristics of H4 and H3 described above, a model of magma mixing may be constructed and some time constraints on the process may be set.

Several major elements in all H4 and H3 samples were plotted against SiO_2 in order to construct a simple mixing line. The samples with the highest silica content were selected as the silicic end-members. Since no unmixed representatives of the pure basaltic end-members are known, a best fit line through the samples pointing to a hypothetical basaltic composition was composed. The line was forced through the silicic composition and the resulting best fit lines are shown on Figure 9. The lines show binary mixing for CaO and K_2O, but for Na_2O and Al_2O_3 some deviations occur. The plagioclase settling discussed above is suggested as an explanation for the enrichment of the Na and

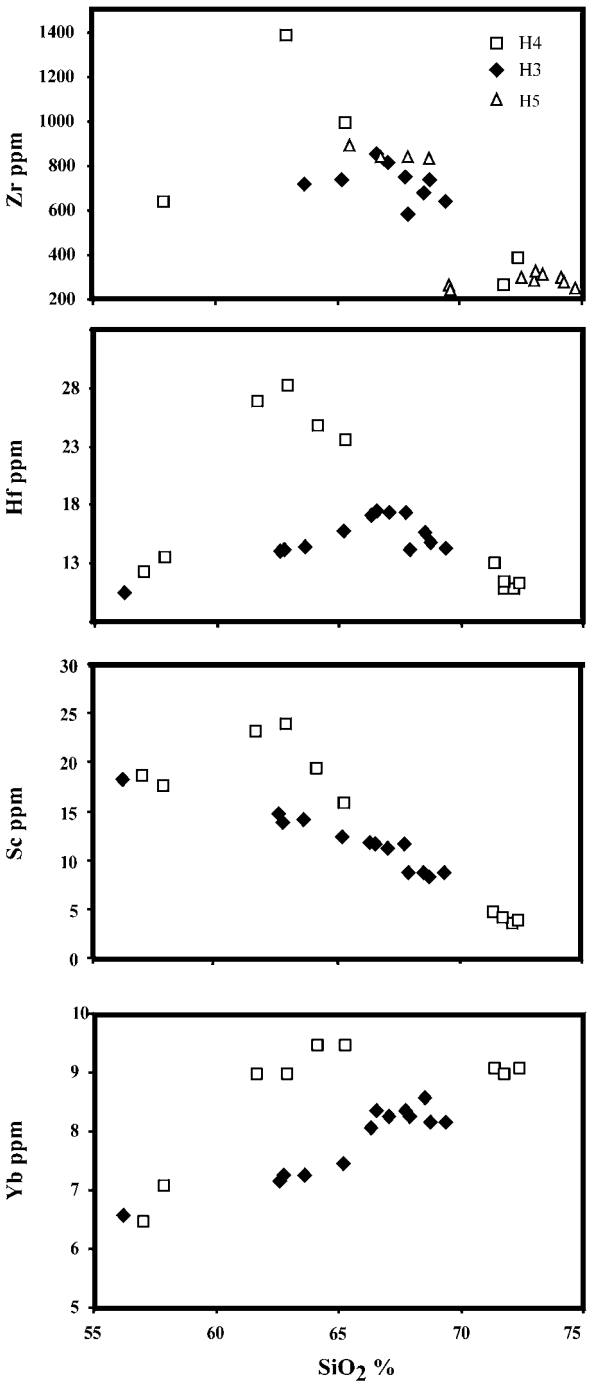

Figure 8. Four trace elements plotted against SiO_2 in the H4 and H3 samples. The elements were selected to demonstrate exceptional enrichment in the hybrid zones in H4. The same elements show more moderate enrichment at higher silica content in H3, and in H5, Zr follows the same trend.

Al in the hybrids, whereas Ca and K would not be affected by crystallization of the oligoclase–andesine compositions. The more evolved characteristics of the H4 silicic magma when compared to the respective H3 magma are also explicitly reflected in Na and Al. The MgO and TiO_2 abundances are mirroring the deviations attributed to plagioclase settling. This is attributed to settling of magnetite, which is the first crystallizing

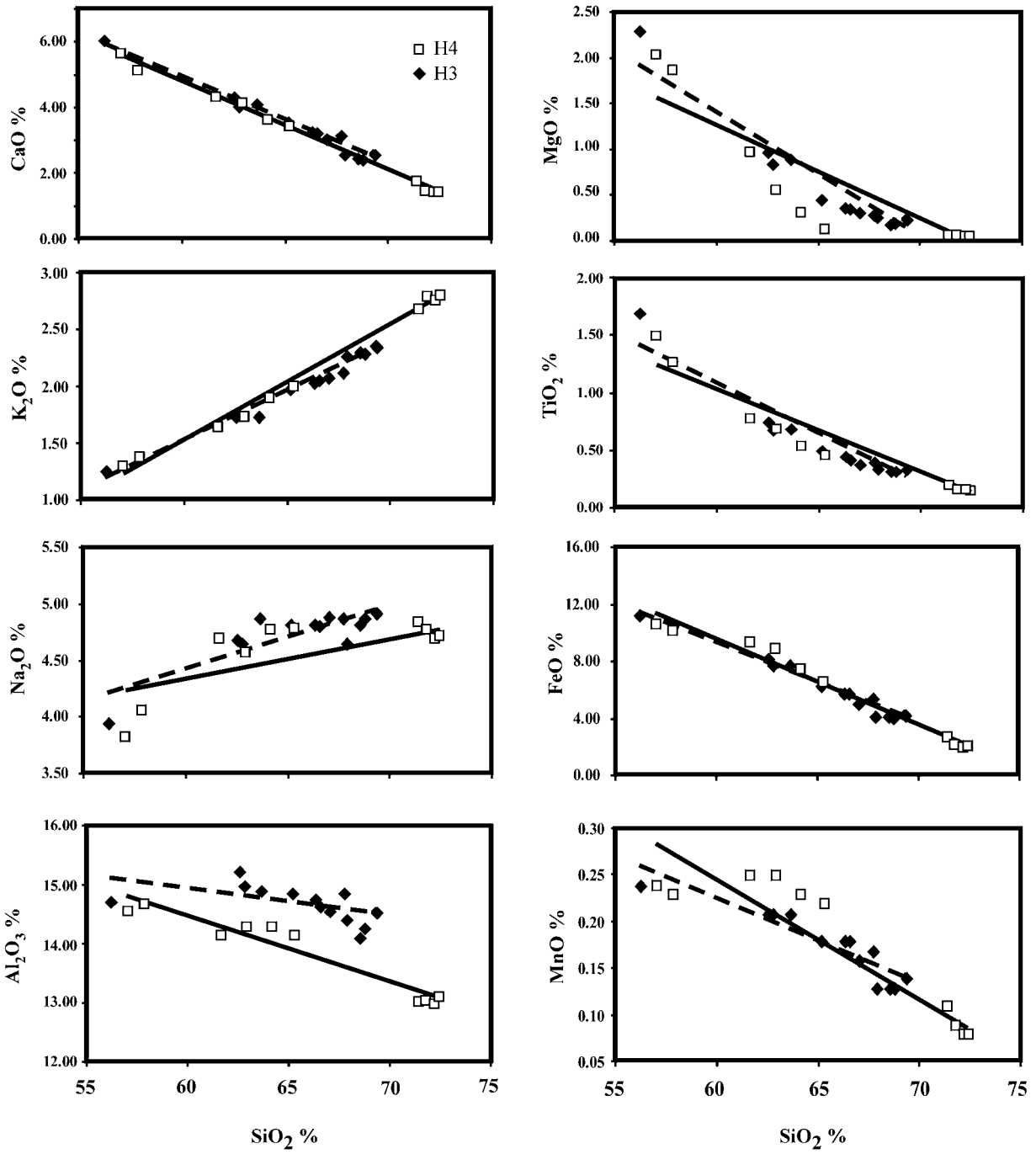

Figure 9. Selected major elements plotted on a Harker diagram for all zones of H3 and H4. Lines are best fit lines forced through the most silicic sample of the respective deposit. Whole line for H4, dashed line for H3.

phase in the rhyolite, according to MELTS calculations (Ghiorso & Sack, 1995). The magnetite has obviously settled further down in the chamber as the deepest zones are enriched, whereas the middle zones are depleted. The faint enrichment in FeO in the middle zones may seem controversial as magnetite is a Fe-rich mineral, but by evidence from the corresponding but amplified enrichment in MnO, it is concluded that the fayalitic olivines found in the rhyolite have settled down to the same depth as the plagioclase. These fingerprints are so decisive that the fact that almost no olivines were found in the hybrids indicates that the crystals were small and had dissolved while the hot basaltic andesite magma mixed with the rhyolites. The absence of small plagioclases probably indicates their dissolution. All these features are explicit in H4 but are also visible to a lesser extent in H3. This confirms that some crystal settling had also started in H3, although not reflected in the crystallinity. It is concluded from mineralogical and chemical evidence that even small-scale crystallization and settling within a magma body puts its clear signature on the compositions. These

observations also imply that the variation in the deposits reflects the almost undisturbed stratification in the magma chamber prior to the eruptions.

The overall chemical gradation of the H4 and H3 deposits indicates a magma mixing process that formed a binary mixture of the silicic magma and a hypothetical basaltic andesite composition without destroying a fine-scale chemical stratification established by pre-mixing crystal settling in the silicic reservoir.

4.c. Mechanism of mixing

4.c.1. Dyke injection

A process that conforms with such a delicate pattern is constrained by several factors. Whether the term 'zonation' is used for these compositional gradients is a matter of definition, as no abrupt changes or clear interfaces are seen between most of the 'zones' in the Hekla products. It is concluded from the uniform composition and equilibrium mineralogy that the rhyolitic magma was almost homogeneous during and after emplacement in the magma chamber, and that nucleation of phases started soon after emplacement. Important supporting evidence for crystal settling in the silicic end-member before mixing is that, in the H5 deposit, which appears to be unmixed rhyolite–dacite, settling of mineral phases had already started. This is confirmed by the Zr anomaly in the less-evolved part of that fallout (Figs 6, 8). This puts some time constraints on the evolution within the silicic reservoir, implying that the crystallization occurred before the basaltic andesite injection. The homogeneous composition of glass within zones, along with the disequilibrium mineralogy, indicates that the mixing was very effective within each level, and that the time between injection and eruption was too short to allow significant growth of equilibrium minerals in the hybrid magma. Nevertheless, some resorption and growth of reversed zoning on the plagioclases entrained with the silicic end-member, and the complete dissolution of smaller crystals had enough time to occur. This indicates that residence time after mixing was short.

Liquidus temperatures were calculated using the MELTS program (Ghiorso & Sack, 1995) for all H4 and H3 samples, and plotted against SiO_2 (Fig. 10). A mixing line was constructed in the same way as for the elements. Most of the calculated temperatures for the hybrids plot slightly above the mixing line, which indicates that mixing will drive crystallization in the hybrid magma. This conforms with the reversed zoning of the phenocrysts. The lowermost hybrid zones plot slightly below the mixing line, which could indicate super-heating of a few degrees. This is consistent with the increasing resorption of crystals at that depth. Since the basaltic andesite end-member is of unknown composition, the exact location of the mixing lines for the basaltic andesite field is less significant.

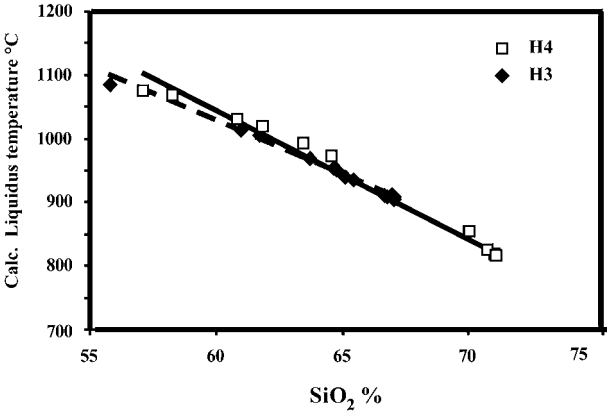

Figure 10. Calculated liquidus temperatures for the H4 and H3 samples, plotted against SiO_2. Calculations were done by the MELTS program (Ghiorso & Sack, 1995). Lines are best fit lines forced through the most silicic sample of the respective deposit. Whole line for H4, dashed line for H3.

Injection of hotter basaltic andesite magma into the residing silicic magma and their intimate mixing conforms well with characteristics of the H4 and H3 fallout. Both magmas are clearly divided into an unmixed part situated in the topmost part of the reservoir, and a lower part forming a range of hybrid compositions. This suggests that the injection of basaltic andesite gradually mixed with the resident silicic magma up to a defined level. Chemical and mineralogical observations can be explained by a fountain mechanism in a magma chamber as described by Campbell & Turner (1989). The critical height reached by an intruding fountain in a resident magma depends on several factors which are not easily measured, such as width of the feeder, and the injective force of the incoming magma. However, as long as the inflow is turbulent, resident magma is entrained into the rising fountain and a stratified hybrid layer is formed.

The shape and size of a magma chamber are also critical factors affecting the mixing process. Clemens & Petford (1999) conclude that tectonics and local structures are more determinative factors for magma emplacement styles than physical properties of the magma, and Eichelberger *et al.* (2000) emphasize that even highly silicic magma is likely to intrude upper crustal reservoirs as dykes. The volcano-tectonics of the Hekla volcano (Gudmundsson *et al.* 1992), as well as the prolonged volcanic activity along this tectonic lineament (Johannesson & Saemundsson, 1989), lend strong support to a dyke emplacement model. There are no signs of local tectonic subsidence, and the absence of hydrothermal activity excludes a shallow magma chamber and shallow plutons. Crustal spreading at the margin of the propagating rift is probably the process that creates space for the magma reservoir of Hekla, along with the effect of the South Iceland seismic zone, which intersects the propagating rift at

this location. Evidence from other regions suggests that crustal spreading creates elongate magma reservoirs (Bjoernsson *et al.* 1977).

A propagating rift model for the volcanic zone in South Iceland is consistent with geodetic GPS studies, which suggest 'tapering' of spreading southwards along the eastern volcanic zone. The spreading rate was estimated to be 8 mm a^{-1} on a profile south of Hekla, compared to a rate of 19 mm a^{-1} on a profile crossing the eastern rift zone 50 km to the north (LaFemina *et al.* 2005).

It is suggested that the magma displacement events, both the segregation of the silicic magma, and the injection of the basaltic andesitic magmas, are driven by periodic crustal spreading. This implies that the mixing events were short-lived injections as described in the fluid dynamics model. Another implication is that the rhyolitic chamber was actually expanding during the injection. The most likely crustal deformation process is upward migration of the whole magma body, causing inflation similar to that which preceded recent eruptions (Kjartansson & Gronvold, 1983; Sturkell *et al.* 2006) but on a larger scale. The basaltic andesite injection may thus be modelled as a dyke which penetrated through the rhyolitic magma, produced hybrid magma by mixing, and finally triggered eruptions.

4.c.2. The magma chamber

The assumption that the magma chamber was completely drained in each eruption only holds for a hypothetical chamber containing the silicic magma and the hybrid magma. Whether the basaltic andesite magma which intrudes the silicic reservoir resides in the 'bottom' of the same reservoir, or if there exist some kind of a 'double chambers' (Gudmundsson, 1988), is uncertain. A dyke-formed magma chamber could also contribute to an explanation of the fact that the stratification was not disturbed by eruption withdrawal (Blake & Fink, 1987).

Frequent dyke injections continued after H3, gradually building the Hekla ridge, but with a successively decreasing contribution from the silicic source. After the last silicic eruption which occurred in AD 1158, approximately two eruptions every 100 years produced less than 10 % of dacite of up to 63 % SiO_2 each, and 90 % basaltic andesite. Compositional range of these eruptions is 54 to 63 % SiO_2 (Table 4). The increased frequency and smaller size of eruptions dominated by basaltic andesite composition could mark a new epoch in the influence of rift propagation on Hekla. A hypothetical model of the Hekla magma chamber from its early formation before the H5 eruption until recent conditions is suggested (Fig. 11a–c).

The time-dependent evolution of the Hekla magmas in the last 1000 year period, as described by Thorarinsson (1967), involves a positive correlation between the SiO_2 content of the initial phase of eruptions and the repose time of the volcano. Evaluation of this observation according to the present model leads to the conclusion that the real time-dependent process is the segregation and accumulation of the

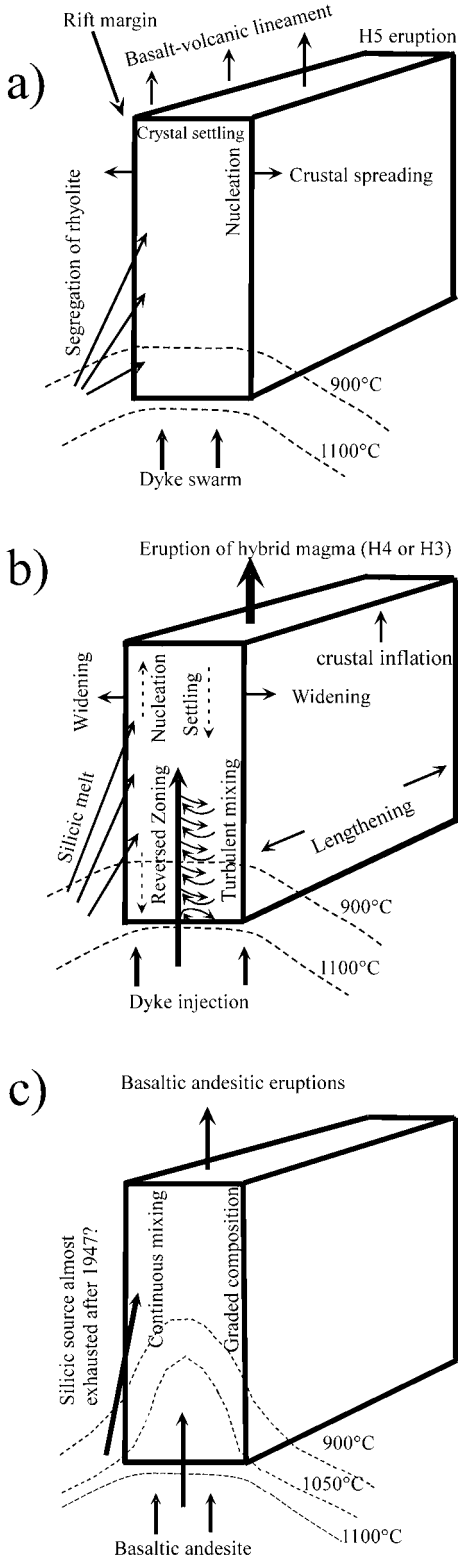

Figure 11. (a–c) Model of the Hekla magma chamber. (a) Suggested formation of silicic reservoir, until the H5 eruption. (b) The large silicic eruptions H4 and H3. (c) Possible evolution in the last 1000 year period.

silicic end-member. Assuming that the injection of the basaltic andesite is driven by crustal spreading as it is for most rift-zone volcanoes, the available quantity of the shallower silicic end-member will be intruded by basaltic andesite during rifting episodes. The mixing process forming the eruptions in the period from AD 1947 back to about 1000 years ago is similar to that described here, except that the end-member proportions are different; the estimated component of the silicic magma is less than 5 %. The last four Hekla eruptions (since 1970) occur after short repose periods (10–20 years) which are apparently too short for significant segregation of silicic melts.

Crustal deformation measurements across the eastern rift zone (ERZ) and western rift zone (WRZ) (Fig. 1) were performed using geodimeters in the years 1967 to 1986 (Decker, Einarsson & Mohr, 1971), and by GPS technique from 1986 to 1994 (Jonsson, Einarsson & Sigmundsson, 1997). These measurements, combined with the history of rifting episodes in south Iceland, indicate more crustal extension across the eastern rift zone than across the subparallel western rift zone during the last 1000 years than during the rest of Holocene time (Sigmundsson *et al.* 1995; Jonsson, Einarsson & Sigmundsson, 1997). This supports the theory that spreading in south Iceland is presently focused on the eastern rift zone, but is not conclusive on the long term partitioning of the activity of the two overlapping rift zones.

The apparent increased production of basaltic andesite in Hekla during the last 1000 year period is consistent with increased activity of the propagating rift.

5. Concluding remarks

The main conclusions of the study of chemical gradation of the two Hekla tephra layers H4 and H3 can be summarized in three stages of magmatic evolution.

Stage 1. Old tholeiitic crust was reactivated by heat flow within a propagating rift; silicic magma formed by partial melting of the crust, segregated and collected in a dyke-formed chamber at considerable depth.

Stage 2. The silicic magma started to crystallize and settle out crystals, but before the phenocryst content reached the average level of 5 %, basaltic andesite magma intruded the chamber from below and mixed with the resident magma, forming a sequence of hybrid magmas.

Stage 3. Eruption was triggered and the pristine rhyolite erupted first, followed by the hybrid compositions. This course of events was probably repeated prior to all Hekla eruptions producing variable compositions.

It is also concluded that the basaltic andesite, which is defined as the mafic end-member of mixing, was not erupted in these two eruptions, but became more common in later eruptions as the proportion of silicic magma diminished.

Availability of silicic magma within the Hekla system is time-dependent, while the injection frequency of basaltic andesite occurs in response to crustal spreading. The result is displayed in a sequence of hybrid eruptions composed of different proportions of similar end-members. Exceptions are the first silicic eruption (H5) where probably unmixed silicic magma was erupted, and the four last eruptions where almost unmixed basaltic andesite has erupted with intervals too short for significant segregation of the silicic end-member.

Intermediate hybrid rocks occur frequently within the Torfajökull centre east of Hekla, where magma mixing between tholeiitic basalts and rhyolite is confirmed (McGarvie *et al.* 1990; Gunnarsson, Marsh & Taylor, 1998). In the Krafla volcanic centre the intermediate rocks are also hybrids of tholeiite and rhyolite (Jonasson, 1994). Hekla is by no means unusual in having magma mixing. However, production of basaltic andesite is not common within the Icelandic rift system. Basaltic andesite, with higher Fe and lower Al than in intermediate rocks, in general, was given the name 'Icelandite' by Carmichael (1964). It is indeed a rare rock type on a global scale, but occurs, for example, in some volcanic centres in Iceland, and in a propagating rift environment in the Galapagos islands (McBirney & Williams, 1969). In Icelandic volcanoes it is produced during a short-lived stage in their evolution. It is inferred that Hekla is undergoing that stage of evolution. The high proportion of basaltic andesite magma in Hekla, compared to many other Icelandic volcanoes, may reflect its tectonic setting on a propagating rift margin. The rare occurrence of this rock type worldwide may be explained by the fact that the tectonic conditions which are favourable to its production are relatively restricted in time and space during the evolution of a propagating rift into older crust.

Acknowledgements. I am grateful to many people who have provided assistance during this work. Gudmundur E. Sigvaldason gave valuable advice in planning the project. Gudrún Larsen did the detailed sampling work, and Susan Russell-Robinson made the WR trace-element analyses. Karl Grönvold helped with the microprobe analytical work. Níels Óskarsson is thanked for valuable help through the course of this work, both as regards practical advice on the chemical and petrological work, and constructive discussions. Amy E. Clifton kindly read the manuscript and improved the English, and gave several useful comments. Rósa Ólafsdóttir provided help with the graphic work. Jón Örn Bjarnason is thanked for continuing encouragement.

References

BALDRIDGE, W. S., MCGETCHIN, T. R., FREY, F. A. & JAROSEWICH, E. 1973. Magma evolution of Hekla, Iceland. *Contributions to Mineralogy and Petrology* **42**, 245–58.

BJOERNSSON, A., SAEMUNDSSON, K., EINARSSON, P., TRYGGVASON, E. & GROENVOLD, K. 1977. Current rifting episode in North Iceland. *Nature* **266**, 318–23.

BLAKE, S. & FINK, J. H. 1987. The dynamics of magma withdrawal from density stratified dyke. *Earth and Planetary Science Letters* **85**, 516–24.

BUNSEN, R. 1851. Ueber die Processe der vulkanischen Gesteinbildung Islands. *Poggendorffs Annalen* **83**, 197–272.

CAMPBELL, I. H. & TURNER, J. S. 1989. Fountains in Magma Chambers. *Journal of Petrology* **30**(4), 885–923.

CARMICHAEL, I. S. E. 1964. The Petrology of Thingmúli, a Tertiary volcano in eastern Iceland. *Journal of Petrology* **5**, 435–60.

CLEMENS, J. D. & PETFORD, N. 1999. Granitic melt viscosity and silicic magma dynamics in contrasting tectonic settings. *Journal of the Geological Society, London* **156**, 1057–60.

DECKER, R. W., EINARSSON, P. & MOHR, P. A. 1971. Rifting in Iceland; new geodetic data. *Science* **173**, 530–3.

DUGMORE, A. J., COOK, G. T., SHORE, J. S., NEWTON, A. J., EDWARDS, K. J. & LARSEN, G. 1995. Radiocarbon dating tephra layers in Britain and Iceland. *Radiocarbon* **37**(2), 379–88.

EICHELBERGER, J. C., CHERTKOFF, D. G., DREHER, S. T. & NYE, C. J. 2000. Magmas in collision: Rethinking chemical zonation in silicic magmas. *Geology* **28**, 603–6.

EINARSSON, T. 1950. *Chemical Analyses and Differentiation of Hekla's Magma. The eruption of Hekla 1947–1948, 4*. Reykjavík: Societas Scientarium Islandica, pp. 1–34.

FURMAN, T., FREY, F. A. & MEYER, P. S. 1992. Petrogenesis of evolved basalts and rhyolites at Austurhorn, southeastern Iceland: the role of fractional crystallization. *Journal of Petrology* **33**, 1405–45.

GHIORSO, M. S. & SACK, R. O. 1995. Chemical mass transfer in magmatic processes IV. A revised and internally consistent thermodynamic model for the interpolation and extrapolation of liquid–solid equilibria in magmatic systems at elevated temperatures and pressures. *Contributions to Mineralogy and Petrology* **119**, 197–212.

GOVINDARAJU, K. & MEVELLE, G. 1987. Fully Automated Dissolution and Separation Methods for Inductively Coupled Plasma Atomic Emission Spectrometry Rock Analysis. Application to the Determination of Rare Earth Elements. *Journal of Analytical Atomic Spectrometry* **2**, 615–62.

GRONVOLD, K., LARSEN, G., EINARSSON, P., THORARINSSON, S. & SAEMUNDSSON, K. 1983. The Hekla Eruption 1980–1981. *Bulletin of Volcanology* **46**, 349–63.

GUDMUNDSSON, A. 1988. Effect of tensile stress concentration around magma chambers on intrusion and extrusion frequencies. *Journal of Volcanology and Geothermal Research* **35**, 179–94.

GUDMUNDSSON, A., OSKARSSON, N., GRONVOLD, K., SAEMUNDSSON, K., SIGURDSSON, O., STEFANSSON, R., GISLASON, S. R., EINARSSON, P., BRANDSDOTTIR, B., LARSEN, G., JOHANNESSON, H. & THORDARSON, TH. 1992. The 1991 eruption of Hekla, Iceland. *Bulletin of Volcanology* **54**, 238–46.

GUNNARSSON, B., MARSH, B. D. & TAYLOR, H. P. JR. 1998. Generation of Icelandic rhyolites: silicic lavas from the Torfajökull central volcano. *Journal of Volcanology and Geothermal Research* **83**, 1–45.

HANCHAR, J. M. & WATSON, E. B. 2003. Zircon Saturation Thermometry. In *Reviews in Mineralogy and Geochemistry, vol. 53: Zircon* (eds J. M. Hanchar & P. W. O. Hoskin), pp. 89–110. Washington, DC: Mineralogical Society of America.

Henderson P. (ed.) 1984. *Rare Earth Element Geochemistry*. Developments in Geochemistry, 2. Amsterdam: Elsevier, 510 pp.

HILDRETH, W. 1979. The Bishop Tuff: Evidence for the origin of compositional zonation in silicic magma chambers. *Geological Society of America, Special Paper* **180**, 43–75.

HILDRETH, W. 1981. Gradients in Silicic Magma Chambers: Implications for Lithospheric Magmatism. *Journal of Geophysical Research* **86**(B11), 10153–92.

HOSKIN, P. W. O. & SCHALTEGGER, U. 2003. The Composition of Zircon and Igneous and Metamorphic Petrogenesis. In *Reviews in Mineralogy and Geochemistry, vol. 53: Zircon* (eds J. M. Hanchar & P. W. O. Hoskin), pp. 27–55. Washington, DC: Mineralogical Society of America.

HOSKULDSSON, A., OSKARSSON, N., PEDERSEN, R., GRONVOLD, K., VOGFJORD, K. & OLAFSDOTTIR, R. In press. The Millennium Eruption of Hekla in February 2000. *Bulletin of Volcanology*.

JÓHANNESSON, H. & SAEMUNDSSON, K. 1989. *Geological map of Iceland. 1:500 000. Bedrock Geology*. Icelandic Museum of Natural History and Iceland Geodetic Survey, Reykjavík (1st ed.).

JÓNASSON, K. 1994. Rhyolite volcanism in the Krafla central volcano, north-east Iceland. *Bulletin of Volcanology* **56**, 516–28.

JONSSON, S., EINARSSON, P. & SIGMUNDSSON, F. 1997. Extension across a divergent plate boundary, the Eastern Volcanic Rift Zone, south Iceland, 1967–1994, observed with GPS and electronic distance measurements. *Journal of Geophysical Research* **102**, 11913–29.

KJARTANSSON, E. & GRONVOLD, K. 1983. Location of a Magma Reservoir beneath Hekla Volcano, Iceland. *Nature* **301**, 139–41.

LAFEMINA, P. C., DIXON, T. H., MALSERVISI, R., ARNADOTTIR, T., STURKELL, E., SIGMUNDSSON, F. & EINARSSON, P. 2005. Geodetic GPS measurements in south Iceland: Strain accumulation and partitioning in a propagating ridge system. *Journal of Geophysical Research* **110**, B11405, doi:10.1029/2005JB003675.

LARSEN, G. & THORARINSSON, S. 1977. H4 and Other Acid Hekla Tephra Layers. *Jökull* **27**, 28–46.

LE BAS, M. J., LE MAITRE, R. W., STREIKEISEN, A. & ZANETTIN, B. 1986. A chemical classification of volcanic rocks based on the total alkali-silica diagram. *Journal of Petrology* **27**, 745–50.

MCBIRNEY, A. R. & WILLIAMS, H. 1969. Geology & Petrology of the Galapagos Islands. *Geological Society of America Memoir* **118**, 1–197.

MCGARVIE, D. W., MACDONALD, R., PINKERTON, H. & SMITH, R. L. 1990. Petrogenetic Evolution of the Torfajokull Volcanic Complex, Iceland, II. The Role of Magma Mixing. *Journal of Petrology* **31**, 461–81.

NORRIS, K. & CHAPPELL, B. W. 1977. X-ray florescence spectrometry. In *Physical Methods in Determinative Mineralogy, 2nd ed*. (ed. J. Zussman), pp. 201–72. London: Academic Press.

OSKARSSON, N., SIGVALDASON, G. E. & STEINTHORSSON, S. 1982. A dynamic model of rift zone petrogenesis and the regional petrology of Iceland. *Journal of Petrology* **23**, 28–74.

ROBINSON, D. M., MILLER, C. F. & AYERS, J. C. 1997. Investigating magma chamber dynamics through the examination of accessory minerals; the Aztec Wash Pluton, southern Nevada. *Abstracts with Programs, Geological Society of America* **29**, 391.

ROELANDS, I. 1977. Neutron activation determination of twenty-one trace elements, including rare-earths, in two ANRT geochemical reference samples: Diorite DR-N and Granite GS-N. *Geostandards Newsletter* **1**, 7–9.

SIGMARSSON, O., CONDOMINES, M. & FOURCADE, S. 1992. A detailed Th, Sr and O isotope study of Hekla: differentiation processes in an Icelandic Volcano. *Contributions to Mineralogy and Petrology* **112**, 20–34.

SIGMARSSON, O., HÉMOND, C., CONDOMINES, M., FOURCADE, S. & OSKARSSON, N. 1991. Origin of silicic magma in Iceland revealed by Th isotopes. *Geology* **19**, 621–4.

SIGMUNDSSON, F., EINARSSON, P., BILHAM, R. & STURKELL, E. 1995. Rift-transform kinematics in south Iceland: Deformation from Global Positioning System measurements, 1986 to 1992. *Journal of Geophysical Research* **100**(B4), 6235–48.

SIGURDSSON, H. & SPARKS, R. S. J. 1981. Petrology of Rhyolitic and Mixing Magma Ejecta from the 1875 Eruption of Askja, Iceland. *Journal of Petrology* **22**, 41–84.

SIGVALDASON, G. E. 1974. *The Petrology of Hekla and Origin of Silicic Rocks in Iceland. The eruption of Hekla 1947–1948, 5*. Reykjavík: Societas Scientarium Islandica, pp. 3–44.

SOOSALU, H. & EINARSSON, P. 2004. Seismic constraints on magma chambers at Hekla and Torfajökull volcanoes, Iceland. *Bulletin of Volcanology* **66**, 276–86.

SPARKS, R. S. J., HUPPERT, H. E. & TURNER, J. S. 1984. The fluid dynamics of evolving magma chambers. *Philosophical Transactions of the Royal Society of London, Series A: Mathematical and Physical Sciences* **310**, 511–34.

STUIVER, M., REIMER, P. J., BARD, E., BECK, J. W., BURR, G. S., HUGHEN, K. A., KROMER, B., MCCORMAC, F. G., V. D., PLICHT, J. & SPURK, M. 1998. *Radiocarbon* **40**, 1041–83.

STURKELL, E., EINARSSON, P., SIGMUNDSSON, F., GEIRSSON, H., OLAFSSON, H., PEDERSEN, R., DE ZEEUW-VAN DALFSEN, E., LINDE, A. T., SACKS, S. I., STEFANSSON, R. 2006. Volcano geodesy and magma dynamics in Iceland. *Journal of Volcanology and Geothermal Research* **150**, 14–34.

THORARINSSON, S. 1967. *The Eruptions of Hekla in Historical Times. A Tephrochronological Study. The eruption of Hekla 1947–1948, 1*. Reykjavík: Societas Scientarium Islandica, pp. 1–170.

THORARINSSON, S. & SIGVALDASON, G. 1972. The Hekla Eruption of 1970. *Bulletin of Volcanology* **36**, 1–20.

TOMASSON, J. 1967. Hekla's magma. In *Iceland and Mid-Ocean Ridges* (ed. S. Björnsson), pp. 180–9. *Societas Scientarium Islandica* **38**. Reykjavík.

TRYGGVASON, T. 1965. *Petrographic Studies on the Eruption Products of Hekla 1947–1948. The eruption of Hekla 1947–1948, 4*. Reykjavík: Societas Scientarium Islandica, pp. 1–13.